

1 Enzymatic mediated modification of gum Arabic by
2 curcumin oxidation products: physicochemical and
3 self-assembly study

4 Aurélie A. Adam, Jordane Jasniewski, Marie E. Vuillemin, Blandine Simard, Jennifer
5 Burgain, Régis Badin, Lionel Muniglia and Florentin Michaux*
6 Université de Lorraine, LIBio, F-54000 Nancy, France

7 * Corresponding author: florentin.michaux@univ-lorraine.fr

8

9 Highlights:

- 10 - The laccase assisted modification of gum Arabic by curcumin oxidation allowed the
11 grafting of phenolic compounds.
12 - Contrary to the native one, modified gum Arabic presented a phase transition
13 temperature.
14 - Due to a higher hydrophobicity, modified gum Arabic formed spherical particles in water.

15 ABSTRACT: Gum Arabic (GA) is a polysaccharide widely used in industry as an emulsifier
16 and encapsulating agent. Nevertheless, its physicochemical properties can be largely
17 improved. The objective of this study was then to modify its structure to improve its
18 functionalities or to provide new ones. To do so, a heterogeneous catalysis process using a
19 laccase and a phenolic compound, curcumin, in aqueous solution was performed. The laccase
20 allowed the oxidation of curcumin, which was then able to be grafted onto the polymer.
21 Therefore, this environmentally friendly process allowed the modification of GA with

22 curcumin oxidation products (OXP) by creating ester bonds between GA and OXP. The
23 molecular mass of GA was largely increased after functionalization. This product contained
24 two fractions of approximately $\sim 1.165 \times 10^8 \text{ g}\cdot\text{mol}^{-1}$ and $\sim 5.057 \times 10^6 \text{ g}\cdot\text{mol}^{-1}$. All these
25 modifications impacted greatly the polymer properties such as its thermal behaviour, with a
26 significant decrease of its glass transition, its hydrophilicity and its hygroscopicity. They also
27 brought antioxidant properties to the modified GA. Moreover, the modification led
28 interestingly to the spontaneous formation of spherical monodisperse micrometric particles in
29 water.

30 KEYWORDS: gum Arabic, curcumin, self-assembly, thermal behaviour, phenol grafting,
31 laccase

32

33 **1. Introduction**

34 Gum Arabic (GA), also known as Acacia gum, is a complex polysaccharide exuded by
35 acacia trees such as *Acacia senegal* and *Acacia seyal* to protect themselves against insects and
36 heal their wounds (Lopez-Torrez, Nigen, Williams, Doco, & Sanchez, 2015; Osman,
37 Williams, Menzies, & Philips, 1993; Verbeken, Dierckx, & Dewettinck, 2003). It was already
38 used 70 000 years ago in Africa and by the Egyptians more than 4000 years ago (Renard,
39 Garnier, Lapp, Schmitt, & Sanchez, 2012; Sanchez et al., 2018; Sanchez, Renard, Robert,
40 Schmitt, & Lefebvre, 2002). Nowadays, GA, thanks to its remarkable properties (high
41 solubility in water), is used as a stabilizer or an emulsifier under the European code E414
42 according to the European food safety authority (EFSA) (Masuelli 2013; Mortensen, Aguilar,
43 Crebelli, Domenico, & Frutos, 2017; Sanchez et al. 2018). It is a common ingredient in
44 confectionery to delay the crystallization of sugar or in wine to prevent pigment precipitation.
45 It is also used in non-food industries, for example as an ingredient in the micro-encapsulation

46 process for the production of carbonless paper (Dickinson, Murray, Stainsby, & Anderson,
47 1988; Osman et al., 1993; Sanchez et al., 2018).

48 GA is a highly branched polysaccharide and is composed of main chains of 1,3 linked β -
49 D-galactopyranosyl. The side chains are composed of β -D-galactopyranosyl linked to the
50 main chain in 1,6. Both chains contain α -L-arabinofuranosyl and α -L-rhamnopyranosyl while
51 most of the β -D-glucuronopyranosyl and 4-O-methyl- β -D-glucuroopyranosyl are located at the
52 end of the side chains (Aphibanthammakit, Nigen, Gaucel, Sanchez, & Charlier, 2018; Lopez-
53 Torrez et al., 2015; Masuelli 2013; Verbeken, et al., 2003). The exact chemical composition
54 of GA can vary depending on different conditions: origin, age of trees or climatic conditions
55 (Cozic, Picton, Garda, Marlhoux, & Le Cerf, 2009; Lopez-Torrez et al., 2015; Masuelli
56 2013). Its structure can be separated in three different fractions: arabinogalactan-peptide
57 (AG), arabinogalactan protein (AGP) and glycoprotein (GP), which represent 85-90%, 10%
58 and about 2% of the whole gum, respectively. As suggested by the names of the different
59 fractions, GA also contains a protein part linked to the polysaccharide part by serine and
60 hydroxyproline rich domains. The GP is then the minor fraction but it is the one containing
61 the most proteins, contrary to the AG, which contains the least amount of protein but is the
62 major fraction of the gum. The AGP fraction contains less protein than GP but more than AG.
63 (Lopez-Torrez et al., 2015; Osman et al., 1993; Renard, Lavenant-Gourgeon, Ralet, &
64 Sanchez, 2006; Sanchez et al., 2018).

65 Despite its many functions, GA has certain limitations. Only one fraction (AGP) is
66 currently valued because it is the only one responsible for the ability of GA to stabilize
67 emulsions (Dickinson et al., 1988; Randall, Phillips, & Williams, 1988; Nakauma et al.,
68 2008).

69 In addition, compared to other polysaccharides, GA is not the most effective for
70 emulsions stabilization compared to lemon or beet pectin for example (Wu, Kong, Zang, Hua,
71 & Chen, 2015). Nakauma et al (2008) were able to determine that for a 15% wt water :
72 triglyceride emulsion made by high-pressure homogenisation, a higher concentration of GA
73 was required to form a stable emulsion than with beet pectin or soluble polysaccharides from
74 soybean (Nakauma et al., 2008). Another study showed that emulsions formed by agitation in
75 a rotor stator system by GA, would be less stable than those formed by the gum extracted
76 from *Prosopis alba*; for a similar initial droplet size initially. In addition, the oil/water
77 interface tension decreased less by GA than by this other gum (Vasile, Martinez, Pizones,
78 Judis, & Mazzobre, 2016). However, from its reactive group, it is possible to modify its
79 properties by modification with exogenous molecules. This has already been recorded in the
80 literature on other polysaccharides (Karaki, Aljawish, Humeau, Muniglia, & Jasniewski,
81 2016; Li et al. 2016).

82 GA modifications were then reported. Gum Arabic was functionalized *via* a Maillard
83 reaction with proteins like casein or canola protein to enhance its emulsifying properties
84 (Hou, Wu, Xia, Phillips, & Cui, 2017; Pirestani, Nasirpour, Keramat, Desobry, & Jasniewski,
85 2017). It has also been modified by chemical pathway to form particles as shown by Sarika,
86 James, Kumar, Raj, & Kumary (2015) where the binding of curcumin has shown to change
87 the physicochemical properties of GA. The formation of spherical particles closed to 200 nm
88 of diameter was demonstrated as well as an increase in anticancer properties compared to free
89 curcumin.

90 The latter paper, such as most papers dealing with polysaccharide modification used a
91 chemical pathway to obtain the modified polymer. Softer processes were rarer but still exist.
92 For example, chitosan and pectin were functionalized with phenolic compounds produced by
93 laccase catalyzed oxidation of ferulic acid and ethyl ferulate. The grafting was found to be

94 covalent between carboxyl groups of pectin or the amine groups of chitosan and the oxidation
95 products of the ferulic acid. The polymer hygroscopicity was decreased and hydrophilicity
96 increased because the oxidation products inserted into the pectin backbone increased the
97 space between the polymer chains. A significant improvement in antioxidant properties was
98 also noted in both polysaccharides (Aljawish et al., 2014; Karaki Aljawish, Muniglia,
99 Humeau, & Jasniewski, 2016).

100 GA was also modified through an enzymatic process. A laccase was used to oxidize
101 ferulic acid to form reactive derivatives (oxidation products), which could then react with the
102 functional groups of GA such as amines or carboxylic acids. The resulting modified polymer
103 exhibited a greater ability to reduce the surface tension of water compared to GA. This
104 modification also induced a decrease in the interfacial tension between water and oil, which
105 could lead to improved emulsifying capabilities. Another interesting aspect of this study was
106 the increase of the antioxidant properties of the modified polysaccharide. These modifications
107 also led to structural changes, modification of its water solubility, its thermal behaviour and
108 its colour (Vuillemin et al., 2020).

109 In the present study, a similar procedure was used, based on the enzymatic oxidation of
110 curcumin, which then reacted with the functional groups of GA. Curcumin is already in itself
111 a food-grade compound widely used for its colour but especially for its various properties
112 (antioxidant and anticancer activities). Moreover, it is largely hydrophobic, which could
113 modify the hydrophilic/hydrophobic balance of the GA by increasing the hydrophobicity and
114 thus induce a self-assembly in water. This modification was made in order to modify the
115 physicochemical properties of the GA. This one has indeed a great solubility in water (up to
116 37% at 25 °C) (Sanchez et al. 2018) and grafting an hydrophobic compound such as oxidation
117 products of curcumin would therefore modify its behaviour in aqueous media. Furthermore,

118 phenolic compounds could also bring a certain antioxidant activity to the gum which could be
119 an advantage for the new polymer.

120 The grafting of the oxidation products (OXP) was studied by Fourier transform infrared
121 spectroscopy and SEC-MALS (size exclusion chromatography multi angle light scattering)
122 analysis. The modification of physicochemical properties was analysed by thermogravimetric
123 analysis (TGA), differential scanning calorimetry (DSC) and measurement of surface tension
124 in water and antioxidant properties. The behaviour in water was then studied.

125 **2. Materials and methods**

126 2.1 Materials

127 Gum Arabic (100% w/w) purified Instantgum AA from *Acacia senegal* was a gift from
128 Nexira (France). Curcumin $\geq 65\%$ w/w (Cur) and salt for buffer solution (Na_2HPO_4 , KH_2PO_4)
129 were purchased from Sigma Aldrich (France). Ethanol (analytical grade) was purchased from
130 Carlo Erba (France).

131 The laccase used was Novozym 51003 from Novozymes (BGAsvaerdt, Denmark) which
132 is a fungal phenol oxidase from *Myceliophthora thermophila* produced in *Aspergillus oryzae*.
133 The activity of the laccase stock is expressed in Laccase *Myceliophthora* Units (LAMU). One
134 LAMU is defined as the amount of enzyme that oxidizes 1 micromole of syringaldazine per
135 minute. The laccase activity was $22\,315 \pm 2\,732$ LAMU.g⁻¹. This activity was calculated by
136 oxidation kinetics of syringaldazine and a Bradford titration of proteins.

137 2.2 Methods

138 2.2.1 *Functionalization of Acacia gum by curcumin oxidation products*

139 The method used was adapted from literature (Vuillemin et al., 2020; 2021). 10 g of
140 GA was added in 450 mL of 50 mM phosphate buffer; pH 7.4 and stirred overnight at 4 °C.

141 GA solubility in phosphate buffer is very low but it has been shown that functionalization can
142 be achieved under heterogeneous conditions (Vuillemin et al., 2021; 2020; Aljawish et
143 al.,2012; Karaki, et al., 2016). The resulting dispersion was then heated under stirring to 30
144 °C using a magnetic heating plate. 50 ml of 50 mM curcumin solution in ethanol was then
145 added to the GA dispersion. Then 10.25 LAMU.mL⁻¹ of laccase was added. The reaction was
146 stopped after 1 h by adding 3 volumes (1.5 L) of frozen ethanol and was then kept at -21 °C
147 for 24 h. This procedure also allowed the separation of functionalized and non-functionalized
148 polymers contained in the mixture at the end of the reaction (Vuillemin et al., 2020). Indeed,
149 gum Arabic-oxidized curcumin (GAC) was soluble in a water/ethanol 1:3 mixture, unlike
150 native GA, which precipitated in this solvent. The native GA was then eliminated by
151 centrifugation at 12 100 g for 10 min. The salts from the buffer were distributed between the
152 two phases. Ethanol contained in the supernatant was evaporated by a BUCHI R144 rotary
153 evaporator at a boiling point of 40 °C at 175 mbar (BUCHI SARL, Rungis, France). The
154 sample (water-suspended GAC) was then frozen and freeze-dried for 24 h. The yield was 20 g
155 of functionalized gum for 100 g of native gum. Dialysis (MWCO 10 000 Da from Membrane
156 Filtration Products Inc.) of the freeze-dried sample against pure water was then performed to
157 remove buffer salts and recover pure modified GA referred to GACD to differentiate it from
158 GAC, which was not dialyzed.

159 2.2.2 *Structure of functionalized Acacia gum*

160 Fourier-transform infrared spectroscopy (FTIR) was used to investigate the impact of
161 functionalization on GA chemical structure. The different compounds were analysed in the
162 solid state so that they would not be affected by water absorption in the region of the amide I
163 band (1720-1580 cm⁻¹). Measurements were performed using a Tensor 27 spectrometer
164 equipped with a DTGS detector (Bruker, Germany). The GACD powder was placed on a
165 diamond ATR top-plate (ATR Platinum, Bruker, Germany). Recording was performed with

166 64 scans, 10 kHz scanning, spectra from 400 to 4000 cm^{-1} and 6 cm^{-1} of resolution. The
167 background was measured on air to be subtracted from the raw spectra. The raw data were
168 collected by OPUS software version 7.2 (Bruker, Germany) and then underwent different
169 treatments which were in sequence: extended ATR correction; transmittance to absorbance
170 spectrum conversion; $\text{H}_2\text{O}/\text{CO}_2$ compensation: straight line generation on the blind area of the
171 diamond detector; 9 points smoothing; baseline correction; offset normalization. All the
172 measurements were performed in triplicate. The degree of esterification was calculated using
173 equation 1 (Karaki et al. 2017; Chatjigakis et al. 1998).

174

$$\begin{aligned} 175 \text{ esterification degree} &= \text{peak area at } 1730 \text{ cm}^{-1} / (\text{peak area at } 1730 \text{ cm}^{-1} + \text{peak area at } 1650 \\ 176 \text{ cm}^{-1}) * 100 & \qquad \qquad \qquad \text{Eq (1)} \end{aligned}$$

177

178 2.2.3 *Polymer molecular weight*

179 SEC experiments were performed with a HPLC pump (LC10AD, Shimadzu) coupled to an
180 autosampler (Autosampler VE 2001, Malvern Panalytical) and a multi-detectors system
181 recording UV, light scattering (RALS: right angle light scattering and LALS: left angle light
182 scattering), intrinsic viscosity and refractive index signals (Viscotek TDA305, Malvern
183 Panalytical). Two SEC columns (A4000-A6000, 10 or 13 μm , 8 mm ID x 300 mm, void
184 volume ~ 6 mL, total volume ~ 12.5 mL, Malvern Panalytical) were mounted in series and
185 equipped with a post-column nylon filter (0.22 μm). The columns were equilibrated with
186 DMAC/ H_2O 50:50. The flow rate was 0.1 $\text{mL}\cdot\text{min}^{-1}$ and the temperature was 30 $^\circ\text{C}$. Data
187 were processed with the Omnisec software (v5.12, Malvern Panalytical). The calibration
188 procedure was performed with Bovin Serum Albumin (Sigma) and cross-validations were
189 performed with Dextran 70 kDa standard (Viscotek PolyCal standards, Malvern Panalytical).

190 The refractometer was used as the concentration detector and the refractive index increment
191 value (dn/dc) used to determine the molecular weight was 0.136 mL.g⁻¹ (Grein, Da Silva,
192 Wendel, Tischer, & Sierakowski, 2013). GACD samples were solubilized in the
193 aforementioned buffer at 10 g.L⁻¹ and filtered through a 0.22 µm RC-filter just before
194 injection. All the measurements were performed in triplicate and expressed with mean ±
195 standard deviation.

196 2.2.4 Antioxidant activity

197 The antioxidant activity of GAC and curcumin were determined by carrying out tests
198 of ABTS^{•+} radical scavenging. The method was adapted from Karaki et al., (2016b) and
199 Vuillemin et al., (2020). Solutions of ABTS^{•+} (2.45 mM) were diluted to obtain an
200 absorbance of 0.680 ± 0.02 AU (arbitrary units) at 734 nm. 1 ml of this solution was then
201 added to 10 µL of sample with a concentration ranging from 0.5 to 0.0005% (wt). After
202 incubation at 30 °C for 20 min and colour stabilization, the absorbance was measured at 734
203 nm in a quartz cell. All the measurements were performed in triplicate and expressed with
204 mean ± standard deviation.

205 The percentage of inhibition of the studied molecules was calculated using the
206 equation 2 where: final A was the absorbance of the ABTS^{•+} solution which has reacted with
207 the studied molecule and where initial A was the absorbance of the ABTS^{•+} solution which
208 had not yet reacted. The values were then expressed in EC50 ± standard deviation. This was
209 the concentration for which the molecule of interest inhibits 50% of the ABTS^{•+} radicals.

210

$$211 \text{inhibition (\% ABTS}^{\bullet+} = 1 - (\text{final A} / \text{initial A}) * 100 \qquad \text{Eq (2)}$$

212

213 2.2.5 *Thermal behaviour analysis*

214 Thermogravimetric Analyses (TGA) were performed on GA, GACD and Curcumin to
215 investigate the impact of functionalization on GA thermal stability. The experiments were
216 performed using a thermogravimetric analysis apparatus (TGA 5500, TA Instruments,
217 Waters, France) under N₂ gas. The heating rate was 20 °C.min⁻¹ from 30 °C to 600 °C and the
218 mass of the sample was approximately 6 mg ± 2 mg. Raw data were collected and analysed
219 using TRIOS software (TA Instruments, Waters, France) to recover thermograms and their
220 derivatives. Each step of compound degradation was determined using the obtained
221 derivatives. All the measurements were performed in triplicate.

222 Differential Scanning Calorimetry (DSC) was performed to investigate the impact of
223 functionalization on GA thermal behaviour (DSC 250, TA Instruments, Waters, France). 6 ± 2
224 mg of GACD, GA or curcumin were filled in a Tzero hermetic aluminium pan to be analysed
225 (TA Instruments). A Heat-Cold-Heat method was chosen. First, the samples were equilibrated
226 at -50 °C, then heated from -50 °C to 100 °C at 10 °C.min⁻¹ to eliminate the thermal history of
227 the samples. Next, they were cooled to -50 °C at 10 °C.min⁻¹, and finally, heated again to 100
228 °C at 10 °C.min⁻¹. All steps were separated by an isothermal step of 2 min. Data were
229 collected using TRIOS software (TA Instruments), which allowed automatic detection of the
230 T_g (glass transition temperature). All the measurements were performed in triplicate and
231 expressed with mean ± standard deviation.

232 2.2.6 *Hygroscopy*

233 The water sorption isotherm of GA and GACD was performed to determine whether the
234 functionalization had an impact on the hygroscopy of the polysaccharide. The results were
235 obtained by depositing 90 ± 10 mg for GA and 50 ± 10 mg for GACD in the sealed chamber
236 of the dynamic vapour sorption analyser (DVS, Surface Measurement Systems Ltd., London,

237 UK). This weight difference was due to the greater volume taken up by the GACD powder
238 (lower powder density) in the capsule of the machine. The temperature was set at 25 °C. The
239 relative humidity (RH) was first brought as low as possible (approx. 0.1 %) and then
240 increased by 10% steps to 85%. The balancing times for the individual steps were set
241 manually such as: (1) for GACD: 500 min for 0.1%; 200 min for 10 to 60%; 300 min for
242 70%; 500 min for 80% and 250 for 85% and (2) for GA: 800 min for 0.1%; 400 min for 20 to
243 40%; 200 min for 50%; 450 min for 60%; 700 min for 70%; 800 min for 80% and 900 min
244 for 85%. The weights were measured continuously but only the weights at equilibrium were
245 recorded. All the measurements were performed in triplicate and expressed with mean \pm
246 standard deviation.

247 2.2.7 *Preparation of aqueous samples: particle dispersion*

248 GAC was dispersed in ultra-pure water at 0.5 wt.% and stored overnight at 4 °C under
249 stirring. This solution was then diluted in ultra-pure water at a chosen concentration for
250 specific investigations.

251 2.2.8 *Surface tension measurement*

252 The surface tension of GAC dispersions in ultrapure water was measured at 25 °C
253 using a Kruss K100 tensiometer (Krüss, Paris, France) equipped with a Wilhelmy plate. In
254 this method a platinum plate was placed at the water/air interface and allowed the capillary
255 force of the solution to be measured. The data were collected continuously over a maximum
256 duration of 21000 s in order to reach the equilibrium. Before each measurement, the
257 cleanliness of the equipment used was checked by carrying out a measurement on ultra-pure
258 water in order to avoid any interference; a value of $72.5 \pm 0.3 \text{ mN}\cdot\text{m}^{-1}$ had to be reached.

259 The evolution of surface tension as a function of time was modelled using equation 3
260 (Mahfoudhi et al., 2014). This equation provides the equilibrium surface tension value (γ_f) for

261 infinite time. The parameters τ_1 , τ_2 , γ_1 and γ_2 were the one to characterize the decay of the
262 surface tension values. τ_1 corresponded to the migration time of the emulsifier to the interface
263 and τ_2 to the time needed for the reorganization of the molecules at the interphase. γ_1 and γ_2 ,
264 in turn, corresponded to the surface tensions corresponding to these different times. γ
265 represented the surface tension at infinity. t corresponded to the time of the measurement. The
266 measurements were performed in triplicate and expressed with mean \pm standard deviation.

$$267 \quad \gamma = \gamma_f + (\gamma_1 - \gamma_f) \cdot e^{-t/\tau_1} + (\gamma_2 - \gamma_f) \cdot e^{-t/\tau_2} \quad \text{Eq (3)}$$

268

269 2.2.9 Size and electrophoresis mobility measurements

270 Size of GA and self-assembled GAC particles was determined with Zetasizer nano-ZS
271 apparatus (Malvern Panalytical, United Kingdom) equipped with a He/Ne ion laser ($\lambda = 532$
272 nm) in a backscattering configuration (measurement angle was of 173°). The refractive index
273 used for the GAC is 1.47. The refractive index of water is also taken into account (1.33). The
274 analysis model used is general purpose for the size and Smoluchowski for the charge.
275 Experiments were performed at 25°C with an equilibrating time of 120 s in a disposable
276 folded capillary cell (DTS1070, Malvern Panalytical). Measurements were made in triplicate
277 and expressed with mean \pm standard deviation.

278 2.2.10 Morphological study

279 Particles morphology of GAC was visualised by a Hitachi S-4800 Field-Effect
280 scanning electron microscopy (SEM) operating at 1.0 kV with a field emission gun (cold
281 cathode). A droplet of a sample at 0.05 wt.% in ultra-pure water was dropped off onto an
282 aluminium plot and let air-dried at room temperature during 48 h and then coated with carbon.

283 Epifluorescence microscope observations with a LEITZ DMR microscope (Germany) and
284 with an H3 Micfilter were also performed in order to visualize the presence of phenols in the

285 particles. Image capturing was carried out by a monochrome CCD COHU camera and was
286 captured at magnification of $\times 40$ with an ocular magnification of $\times 10$. The excitation
287 wavelength was of 420 nm. Observations were made by smearing a 0.05% aqueous solution
288 of GAC with a magnification $\times 400$ and $\times 1000$ by immersion.

289 Surface structure of freeze-dried particles was recorded using atomic force microscopy
290 (AFM) (Flex-Axiom, Nanosurf, Liestal, Switzerland) with the Nanosurf C3000 controller
291 software. Powders were gently dispersed on a thin layer of epoxy glue spread onto a circular
292 glass slide. Particle surface properties (topography and elasticity) were recorded at 22 ± 2 °C
293 using an AFM cantilever (Stat0.2LauD cantilevers from Nanosurf, Liestal, Switzerland)
294 having a spring constant of 0.2 N.m^{-1} . Topography acquisition was performed in air, in
295 contact mode on a $5 \mu\text{m} \times 5 \mu\text{m}$ surface area. The average surface roughness (S_a) was
296 calculated for single particles on $1 \mu\text{m} \times 1 \mu\text{m}$ according to Equation 4.

$$297 \quad S_a = \frac{1}{n} \sum_{i=1}^n |y_i| \quad \text{Eq (4)}$$

298 where y is the height (z) measured by the piezoelectric scanner at a given pixel (i) in the
299 image. At least 3 particles were analyzed to be able to average the surface roughness value.

300 Mechanical properties of GAC were probed at the nanoscale by AFM nanoindentation
301 technique. The force-distance curves recorded by AFM were analysed according to the
302 theoretical Hertz model to extract the mechanical properties (e.g. elasticity). Defined areas of
303 $5 \mu\text{m} \times 5 \mu\text{m}$ were probed to generate elasticity maps. The cantilever spring constant was
304 calculated thanks to the thermal calibration method and deflection sensitivity calibrated onto a
305 silicon surface. Elasticity maps of 1024 force curves were processed with the ANA Software
306 (Nanosurf, Liestal, Switzerland). At least three topography images and 3 elasticity maps were
307 recorded and analysed.

308 3. Results and discussion

309 3.1 Structure of modified Acacia gum

310 FTIR analyses were performed to evidence changes in the chemical structure of GA
311 induced by the functionalization process. The polymer modification can lead to diverse
312 changes in GA structure observable on FTIR spectra. Polysaccharide modification with the
313 OXP of phenolics compounds can lead to the formation of ester and/or amide bonds. Indeed,
314 the oxidation of phenol by phenol oxidases may lead to the formation of semi-quinones which
315 then react with carboxylic acid groups of glucuronic acid of GA (Lopez-Torrez et al., 2015) to
316 form ester bonds. The protein fraction of GA may also react to form amide bonds with
317 oxidised phenol (Vuillemin et al., 2020). Formation of ester bonds have already been reported
318 between pectin and oxidation products obtained from ferulic acid (Karaki, Aljawish,
319 Muniglia, Bouguet-Bonnet, & Laclerc, 2017). The oxidation of phenols such as tannic acid,
320 quercetin, caffeic acid or gallic acid could lead to the formation of ester or amide bond on
321 polysaccharides such as chitosan (Božič, Gorgieva, & Kokol 2012a; 2012b). Indeed the
322 modification *via* phenol oxidases mediated-system has led to the formation of quinones,
323 which can react with nucleophilic groups such as amines to produce Schiff bases (Aljawish et
324 al., 2014; Kumar, Smith, & Payne 1999).

325 The complete spectra of GACD, curcumin and GA are visible on Figure 1A. The
326 fingerprint of these compounds was found between 1800 and 400 cm^{-1} . A focus on this
327 specific area is presented in Figure 1B.

328 From 3600 to 3000 cm^{-1} the broad band corresponded to the characteristic stretching of O-
329 H and N-H bonds (Božič et al., 2012b; Liu, You, Tarafder, Zou, & Fang 2019). It was
330 possible to see two peaks on the curcumin spectrum, one at 3510 cm^{-1} and the other one at
331 1279 cm^{-1} corresponding to the stretching and the bending of the phenolic -OH groups,

332 respectively (Božič et al., 2012b; Liu et al., Ying, Cai, & Le, 2017; Nascimento da Silva, de
333 Matos Fonseca, Feldhaus, Soares, & Valencia, 2019). Peaks located at 1600 and 1508 cm^{-1}
334 corresponded to the stretching of the C=C bonds of the cyclic alkenes (Božič et al., 2012b;
335 Hasan et al., 2016; Poljanšek, Šebenik, & Krajnc 2006). These peaks were correlated to
336 aromatic rings in curcumin. C-O-C bonds sign at 1026 cm^{-1} corresponding to the COCH_3
337 groups in its structure (Liu et al., 2019; Poljanšek et al., 2006). The peak at 1279 cm^{-1}
338 corresponded to the phenolic C-OH (Liu et al., 2019; Poljanšek et al., 2006)

339 On the spectrum of GA, peaks corresponding to the amide bands I and II at 1649 cm^{-1} and
340 1597 cm^{-1} respectively were visible. The amide III band was located at 1225 cm^{-1} . (Liu et al.,
341 2019; Liu, Cai, Jiang, Wu, & Le, 2016; Lopez-Torrez et al., 2015)

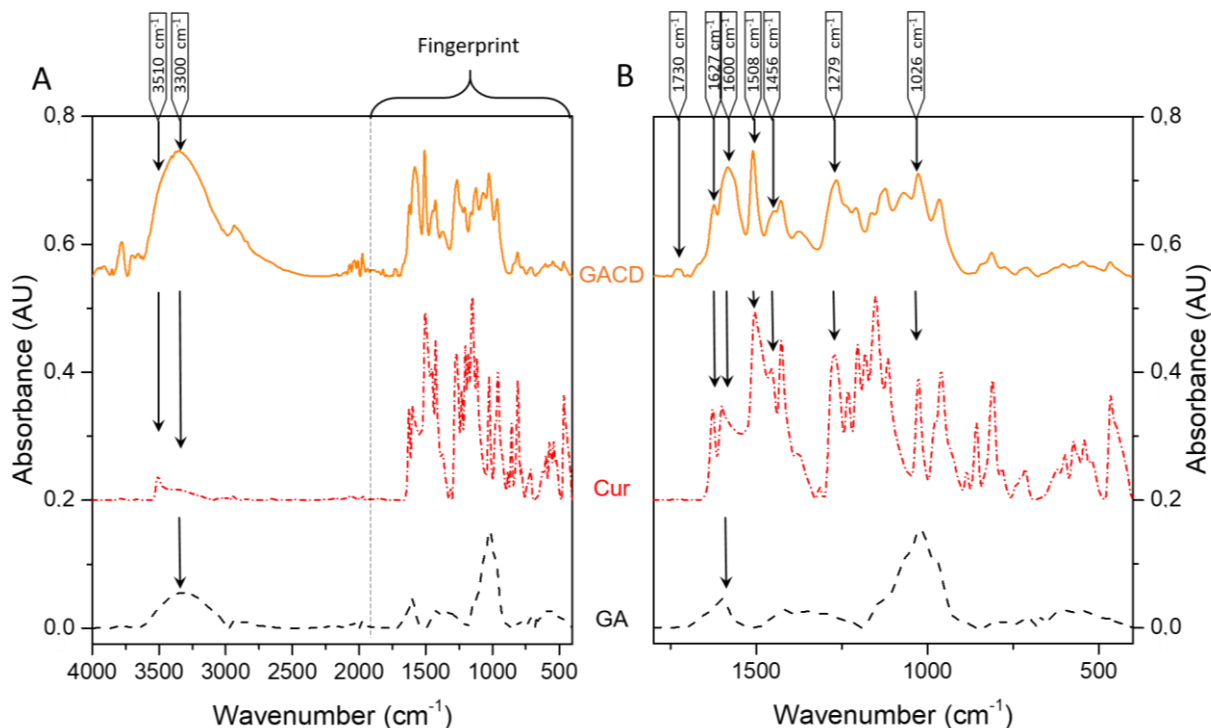
342 On the GACD spectrum the same two peaks as visible on curcumin spectra were reported
343 at 1600 and 1508 cm^{-1} which corresponded to the stretching of the C=C bonds of the cyclic
344 alkenes (Božič et al., 2012b; Hasan et al., 2016; Poljanšek et al., 2006). These peaks
345 suggested that aromatic rings were also present in GACD structure. However, the peak at
346 1600 cm^{-1} was, on GACD spectrum, broadened by the presence of two other peaks and in
347 particular a peak at 1589 cm^{-1} corresponding to the signals of the amide II band (Liu et al.,
348 2019; Liu et al., 2016) indicating the presence of proteins brought by the GA. The amide III
349 band was not clearly visible because it is assigned to a region where too many bonds vibrated.
350 The amide I band was present at 1627 cm^{-1} but this peak also corresponded to the signals of
351 the C=O from curcumin and from COO^- groups notably brought by the polysaccharidic part
352 of the GA (Abdul Rohman, Sudjadi, Devi, Dwiky Ramadhani, & Ardi Nugroho, 2015; Lopez-
353 Torrez et al., 2015; Mundlia, Ahuja, Kumar, & Pillay, 2019).

354 The peak corresponding to the phenolic C-OH at 1279 cm^{-1} on the curcumin spectrum
355 shifted to 1265 cm^{-1} on the GACD spectrum. This change could be induced by the formation

356 of ester bonds since this type of bond brings C-O bonds that stretched asymmetrically at this
357 wave number (Liu et al., 2019; Poljanšek et al., 2006).

358 This hypothesis was correlated by the appearance of a new peak on the GACD spectrum
359 at 1730 cm^{-1} . This peak was characteristic of the stretching vibration of the C=O carbonyl
360 bonds of esterified carboxyl functions (Božič et al., 2012a; 2012a; Karaki et al., 2017; 2017;
361 Vuillemin et al., 2020). There was therefore a combination of clues that an ester bond was
362 formed between the hydroxyl groups of curcumin and the carboxyl groups of GA.

363 The degree of esterification of GACD, calculated from the intensity of the free and
364 esterified carbonyl peaks, was 11.4% whereas it was equal to 2.6% for native GA. The
365 functionalization allowed to esterify 8.8% more of COO^- group. This result should be taken
366 with caution because the presence of the amide I band at the same wavenumber as the
367 carbonyl groups did not allow to evaluate precisely the esterification degree. However, the
368 presence of the amide band suggested that some of the protein fraction of the GA was present,
369 or it may also be possible that bonds were formed between the curcumin OXPs and the
370 proteins, but this cannot be verified here.



371

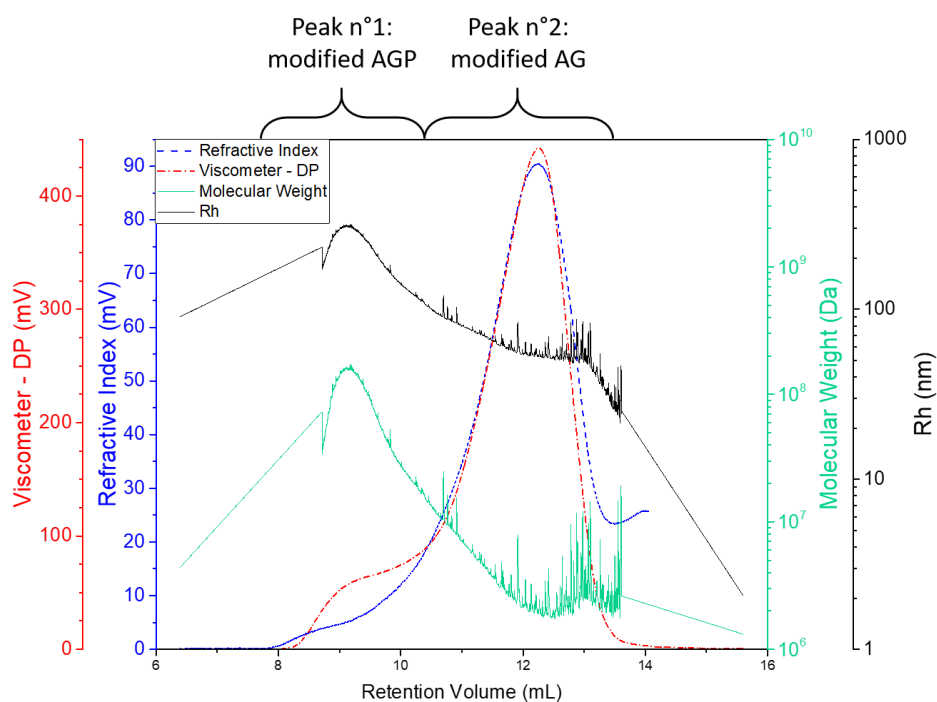
372 Figure 1: (A) FTIR spectra of gum Arabic (GA) (black dash line), of curcumin (Cur) shifted
 373 by 0.2 AU (red dash dot line) and GACD shifted by 0.55 AU (solid orange line); (B) focused
 374 FTIR spectra of GA, Cur and GACD between 600 and 1800 cm^{-1}

375 3.2 Polymer molecular weight

376 The impact of curcumin OXP grafting on the molecular weight and hydrodynamic radius
 377 of GA has been determined using size exclusion chromatography coupled to a multi-detectors
 378 system (UV, LS, IV and RI signals were recorded). GAC was analyzed (Figure 2) and two
 379 peaks were observed, probably corresponding to the modified AGP and AG fractions of 1.249
 380 $\times 10^6 \text{ g}\cdot\text{mol}^{-1}$ (Vuillemin et al., 2021). Indeed, due to the low UV signal at 280 nm, it was
 381 concluded that GP fraction was eliminated during ethanol precipitation realized after the
 382 enzymatic reaction leaving only a purified and functionalized AGP and AG fractions. The
 383 proportion of each fraction was determined using RI detector (2.5% for AGP and 97.5% for
 384 AG). The determination of M_w using light scattering gave M_w of $\sim 1.165 \times 10^8 \text{ g}\cdot\text{mol}^{-1}$ and
 385 $\sim 5.057 \times 10^6 \text{ g}\cdot\text{mol}^{-1}$ for these respective fractions. Finally, the determination of the
 386 hydrodynamic radius (R_h) was performed thanks to IV detector, giving values of ~ 222 and 59

387 nm (see Table S1 in supplementary materials for a summary of the derived parameters).
388 Compared to the native gum Arabic (Vuillemin et al., 2021), the calculated molecular weights
389 of the two fractions of the GAC were very high, suggesting an important grafting of curcumin
390 OXP onto the polysaccharide and probably a crosslinking between the fractions.

391 A very low UV signal at 280 nm was observed, the determination or estimation of the
392 protein content of each fraction was not possible. However, a significant absorbance at 300
393 nm was observed, certainly due to curcumin OXP present on GAC. Surprisingly, no UV
394 signal at 420 nm was observed suggesting the absence of accessible curcumin onto GAC.



395
396 Figure 2: Size exclusion chromatography characterization (refractive index blue dash line,
397 viscometer red dash dot line, M_w green solid line and Rh black solid line) of GAC. AG =
398 arabinogalactan-peptide, AGP = arabinogalactan protein.

399

400 3.3 Antioxidant activity

401 GA is a polymer that contains a small proportion of phenolic compounds such as catechin
402 and gallic acid. These phenols give to the GA a very low antioxidant activity (Hamdani,
403 Wani, Bhat, & Masoodi, 2018; Tahir et al., 2018). Their quantity is so small in relation to the
404 total amount of GA that it shows only a very low antioxidant activity. Its EC50 is around 560
405 g.L⁻¹ according to the literature (Vuillemin et al., 2020). The addition of phenol derivatives
406 improved its antioxidant activity. The EC50 of the GAC was 20.9 ± 0.8 mg.L⁻¹ (about 0.002%
407 wt). The antioxidant activity of the gum was stepped up by 25 000, due to the intake of OXP.
408 In comparison, pure native curcumin, which is well known for its antioxidant activity,
409 presents an EC50 of 3.7 ± 0.5 mg.L⁻¹. The modification of GA from the grafting of
410 antioxidant molecules such as oxidation products of ferulic acid, a structural analogue of
411 curcumin with only one phenolic ring, using a similar pathway as the one use in this study,
412 has already allowed to increase the antioxidant activity of GA to 1.33 g.L⁻¹ (Vuillemin et al.,
413 2020). Using OXP coming from curcumin allowed an even better antioxidant activity.

414 3.4 Thermal analysis

415 Modification of GA with curcumin derivatives modified many physicochemical properties
416 of GA. With this mind, thermal analyses were carried out by TGA and DSC.

417 Thermal stability has been determined to observe the change in GA degradation upon
418 temperature after functionalization. Figure 3 shows the thermograms of GA, GACD and
419 curcumin.

420 The first weight loss recorded before 100 °C corresponded to weakly bound water
421 whereas more strongly bound water was detected up to 150 °C. In this temperature range,
422 different behaviours between the native and the functionalized gum were reported. This first
423 stage of degradation before 150 °C represented about 6 and 3% of their total weight for GA

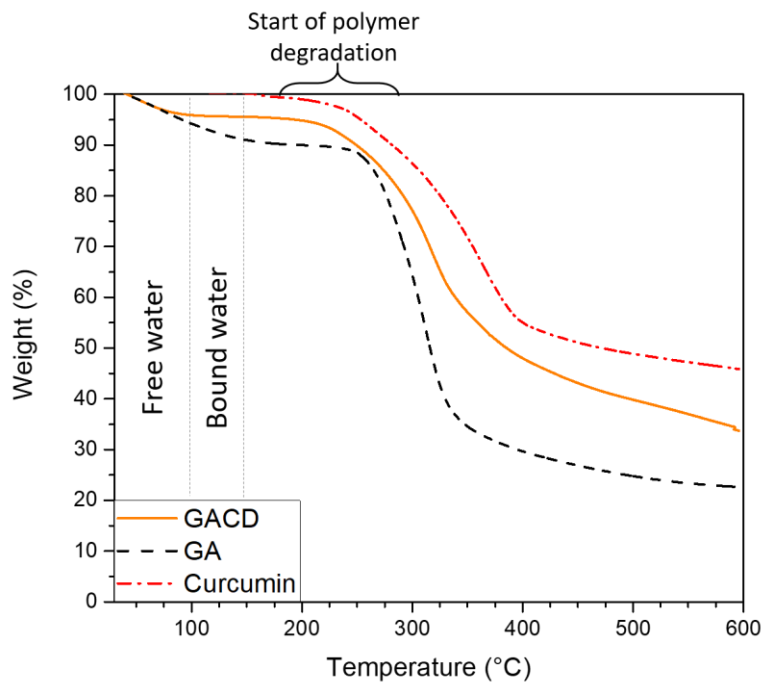
424 and GACD, respectively. Moreover, GACD lost all of its water before 100 °C, whereas GA
425 weight losses were about 6% before 100 °C and 4% between 100 and 150 °C. It seemed then
426 that GACD was relatively less hygroscopic than GA since it contained a lower amount of
427 strongly bound water. GACD was also more hydrophobic than GA because it contained less
428 water, and the greater the degradation step in this temperature range is, the more hydrophilic
429 the polymers are (Zohuriaan & Shokrolahi 2004). These differences could be due to the
430 presence of grafted OXP that would have modified the hydrophilic properties of gum Arabic
431 by increasing its hydrophobicity. This was already noticed by Vuillemin et al., (2020) for gum
432 Arabic modified by oxidation products of ferulic acid. It may also modify the inter-chain
433 spacing of the polymer, giving more space to water adsorption which then modified the
434 hygroscopy. Curcumin contained almost no water without any weight loss below 150 °C. This
435 seemed to make sense since it was a very hydrophobic molecule.

436 A second and more important stage of degradation was observed at higher temperatures.
437 This weight decrease was the greatest for GA (~ 60% of the total weight between 225 °C and
438 400 °C and ~ 40% of the total weight for GACD in the given temperature range) and could
439 correspond to a decomposition step of the polymer. This degradation step showed that GACD
440 was less temperature stable than native GA since it started to degrade before.

441 At 600 °C, at the end of the heating process, more residue remained for GACD (~ 40%)
442 than for GA (~20%). These obtained data with GA have been correlated with those reported
443 in the literature (Cozic et al., 2009; Mothé & Rao 2000; Zohuriaan et al., 2004).

444 Therefore, functionalization had an impact by changing the thermal stability of the
445 polymer. It had already been noted in the literature that the functionalization of gum Arabic
446 modified its temperature stability (Ahmad, Mazumdar, & Kumar 2013; Zohuriaan- Mehr,

447 Motazedi, Kabiri, & Ershad- Langroudi, 2005) and especially its functionalization by
448 phenols (Vuillemin et al., 2020).



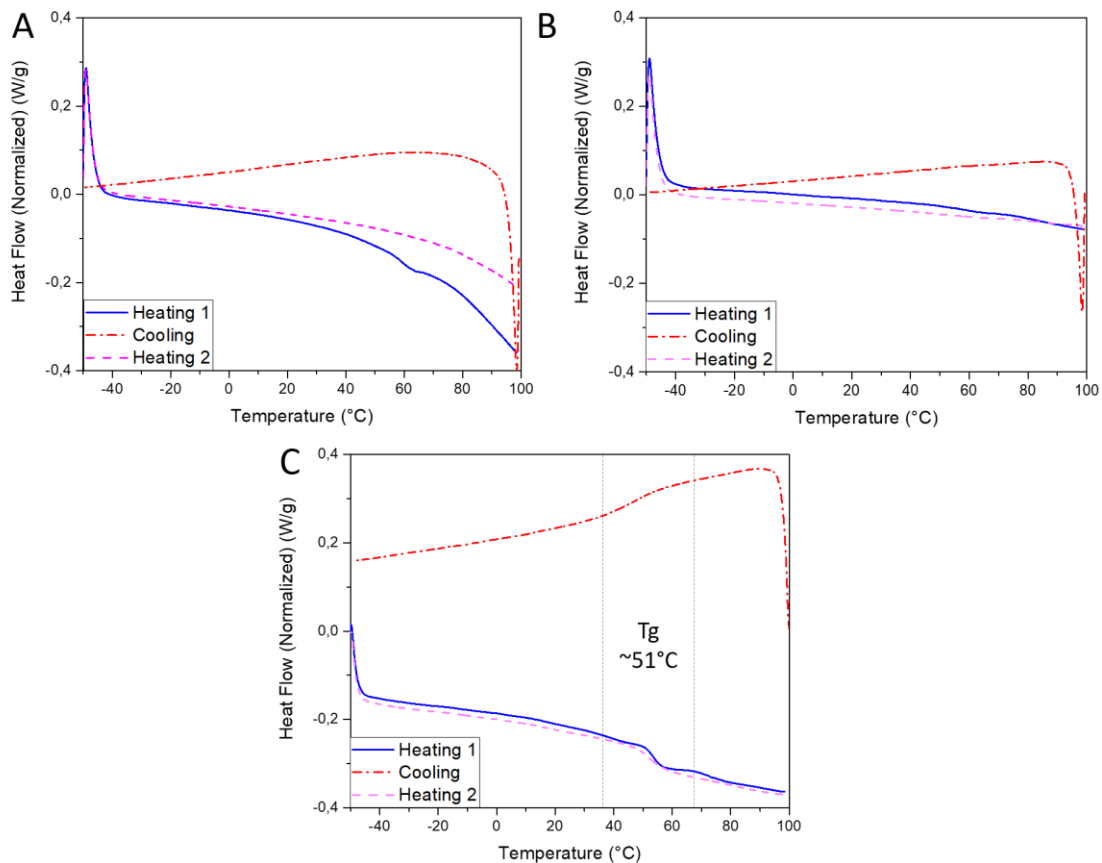
449

450 Figure 3: Thermograms of GA (black dash line), GACD (orange solid line) and Curcumin
451 (red dash dot line) obtained by TGA

452 Thermal behaviour was studied by DSC. GA and curcumin thermogram did not show any
453 significant event in the studied temperature range. It is quite frequent that in the studied
454 temperature range no T_g was detected on the GA thermograms as it has been reported by
455 various authors such as Mothé et al., (2000), Zohuriaan et al., (2004) or Sabet, Rashidinejad,
456 Melton, Zujovic, & Akbarinejad et al., (2021). The difference that can be observed on DSC
457 thermograms closed to 60 °C between the first heating vs. cooling and second heating
458 corresponded to an enthalpic relaxation due to the thermal history of the sample.

459 After functionalization with OXP of curcumin, gum Arabic exhibited a glass transition (a
460 significant endothermic thermal event) at 51 °C ± 7 °C. The presence of this new event
461 suggested that oxidized compounds fixed onto the polysaccharide modified the inter-chain
462 spaces of the polymer by filling steric hindrance. This steric modification allowed gum Arabic

463 to obtain a rubber amorphous state over 51 °C. These type of results were already reported
464 onto pectin or inulin modified by ferulic acid or catechin (Karaki et al., 2016; Spizzirri et al.,
465 2010) and on GA modified by ferulic acid (Vuillemin et al. 2020).



466

467 Figure 4: Thermograms obtained by DSC of (A) GA, (B) Curcumin and (C) GACD with in
468 solid blue line the first heating, in red dash dot line the cooling and in pink dash line, the
469 second heating. T_g : glass transition

470 3.5 Hygroscopy

471 Gum Arabic is a hydrophilic polymer soluble up to $42.5 \pm 2.6\%$ w/v (Vuillemin et al.,
472 2020) and curcumin is an hydrophobic molecule (Peng et al., 2018). By grafting OXP of
473 curcumin, GA seemed to become less hydrophilic and less hygroscopic as suggested by the
474 TGA results. Indeed, modification by hydrophobic compounds such as phenols could modify
475 the affinity of the polysaccharide with water (Karaki et al., 2016). The sorption curves of the

476 GA and GACD were then carried out to determine whether the functionalization changed
477 interaction of modified GA with water (Figure 5).

478 The water sorption isotherm of GA was of type II according to international union of pure
479 and applied chemistry (IUPAC). The part at low relative humidity (RH), corresponded to the
480 strongly bound water related to the hygroscopy of the material. The second part in the middle
481 RH range corresponding to the quasi linear section which matched to the weakly bound
482 multilayer water absorbed by capillarity. The third region (high RH) corresponded to free
483 water (Lykiema, Sing, Haber, Kerker, & Wolfram, 1984). For GA the first part could be
484 between 0.1 and 20% of RH, which would correspond to the water necessary to form a
485 monolayer around the polymer. Multilayer adsorption then starts up till 60%. Above this
486 humidity, only free water is added around the polymer. This behaviour has already been
487 reported by some authors (Frascareli, Silva, Tonon, & Hubinger, 2012; Pérez-Alonso,
488 Beristain, Lobato-Calleros, Rodríguez-Huezo, & Vernon-Carter, 2006).

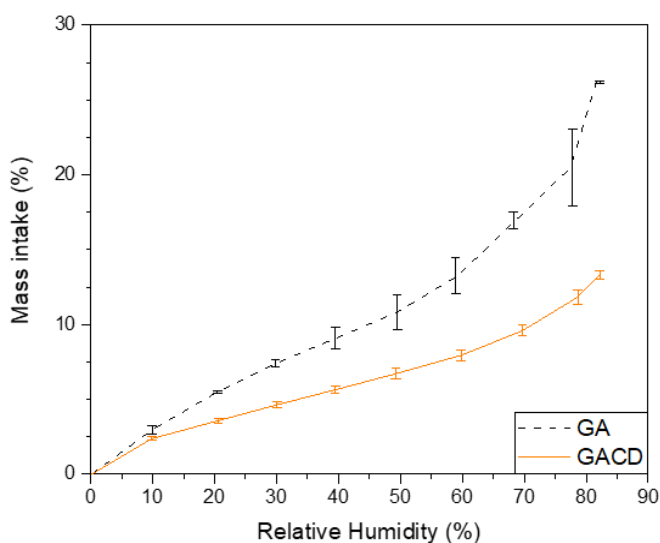
489 The sorption isotherm obtained for GACD was also of type II but was considerably
490 different from GA. The monolayer adsorption of water was terminated at the very latest at
491 10% relative humidity. The formation of multilayer water around the polymer was terminated
492 at 60% and then only free water was added. In addition, less water was adsorbed onto the
493 polymer.

494 The effect of the grafting of phenolic groups could therefore be seen at lower RH since the
495 adsorbed water content was lower, this meant that GACD was less hygroscopic than GA. At
496 high RH the weight intake of GACD was also lower than for GA suggesting that GACD was
497 less hydrophilic than native gum.

498 As previously supposed from TGA experiments, the functionalization due to the addition
499 of OXP, decreased hygroscopy and hydrophilicity. Karaki et al., (2017) were able to show

500 that oxidation product of ferulic acid bound to pectin induced a higher hydrophilicity than
501 native pectin. Authors argued that this result was due to the opening of the structure by the
502 oxidation products creating larger spaces between the chains and allowing more water to be
503 absorbed. In the present case, for GACD, hydrophilicity is lower than that of the native
504 polymer. It is therefore at this stage complicated to affirm something about inter-chain space
505 with absolute confidence. However, it was not the same polysaccharide nor the same phenol
506 that in this study. GA was slightly more hydrophilic and less hygroscopic than pectin.
507 Moreover, thanks to the DSC thermograms, it was possible to show a Tg on the GACD and
508 not on the GA whereas the GA was more hydrophilic and water has a plasticizing effect on
509 polymers. It was then possible to consider that the oxidation products from curcumin were
510 much more hydrophobic and repelled more water and due to this hydrophobicity, the spaces
511 created between the chains were insufficient to accept as much water as the GA. It is also
512 possible that the spaces between the chains were filled with OXP and thus water cannot get
513 into them and these OXP may had a plasticizing effect on GACD, allowing it to exhibit a
514 phase transition.

515 It has also already been shown that the functionalization of gum Arabic could lead to a
516 reduction of its hydrophilicity, in particular through the addition of hydrophobic phenol
517 derivatives (Vuillemin et al., 2020). It has also already been shown on other polysaccharide
518 like chitosan (Aljawish et al., 2016).



519

520 Figure 5 : Water sorption isotherms of GA (black dash line) and GACD (orange solid line)

521

522 3.6 Behavior in water

523 Gum Arabic is a naturally amphiphilic polymer. The grafting of hydrophobic phenolic
 524 compounds has made the GAC more hydrophobic and thus modifying its behavior in water.
 525 Indeed, GA has a natural ability to lower the surface tension of water. Various studies have
 526 been conducted on this subject (Wu et al., 2015; Ebrahimi, Homayouni Rad, Ghanbarzadeh,
 527 Mohammadali, & Pasquale, 2020; Cao, Zhang, Zhang, & Du, 2013; Wang, Williams, &
 528 Senan, 2014; Vuillemin et al., 2020). It is able to lower the water surface tension about 65
 529 $\text{mN}\cdot\text{m}^{-1}$ at a concentration of 0.5% (wt). Once modified by phenols, the GAC lowered even
 530 more the water surface tension. It was then able to lower the water surface tension to $51.6 \pm$
 531 $0.3 \text{ mN}\cdot\text{m}^{-1}$ at 0.5% (wt). A decrease of the surface tension is shown in Figure S1 in
 532 supplementary materials.

533 It has already been shown that modification of GA with hydrophobic compounds
 534 improves the ability of the gum to decrease the surface tension of water (Vuillemin et al.,
 535 2020; Wang et al., 2014). It should also be noted that the ability of GA to decrease surface
 536 tension is primarily due to the AGP fraction (Dickinson et al., 1988; Randall, Phillips, &

537 Williams, 1988; Nakauma et al., 2008). In GAC, the AG fraction is also functionalized and
538 thus could participate in the lowering of surface tension. Functionalization thus allowed the
539 valorisation of an important part of the GA which was not exploited until now.

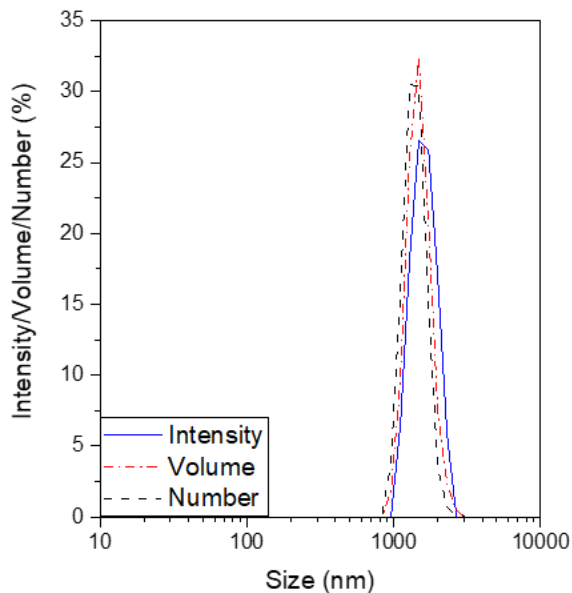
540 The modification of the amphiphilicity of the GA may also induce a self-assembly
541 phenomenon since it depended on the balance between hydrophobic and hydrophilic
542 interactions to minimize energetically unfavourable interactions as reported by Sarika et al.
543 (2015). By increasing the hydrophobicity, the interactions with water were less favourable
544 and therefore the polymer promoted particle formation (Akiyoshi & Sunamoto 1996; Huie
545 2003; Six & Ferji 2019), whereas, for the same concentration, the native polymer was
546 solubilized in water. GAC preparation in water thus led to very turbid sample even at very
547 low concentrations. The presence of this cloudiness indicated the spontaneous formation of
548 particles in water. This behavior had not, to this day, been shown on enzymatically modified
549 GA with phenols such as ferulic acid (Vuillemin et al., 2020). However it has been reported in
550 literature that the polysaccharides chemical modification using phenolic compounds could
551 lead to the formation of particles as demonstrated with pectin and curcumin (Mundlia et al.,
552 2019). It has already also been shown that a chemical grafting of curcumin onto gum Arabic
553 lead to the formation of particles in water composed of an hydrophobic curcumin core and a
554 hydrophilic polysaccharide shell (Sarika et al., 2015). A recent study also shows that dextran
555 enzymatically modified with curcumin could form self-assemblies in water (Curcio et al.,
556 2019) as it is shown today with GA.

557 Measurements of particles hydrodynamic diameter by dynamic light scattering have
558 shown that the size of these particles was in mean 1621 ± 94 nm in diameter. The
559 polydispersity index of the particle size populations was 0.130 ± 0.068 . Size distributions
560 expressed in intensity, volume and number are presented on Figure 6. Peaks were centred at
561 1616, 1496, and 1401 nm for intensity, volume, and number, respectively. Such close values

562 illustrated that the three curves were overlapping suggesting monodisperse size distribution.
563 The polydispersity appeared then to be very low and did not correspond to particles formed
564 by a simple aggregation but rather a self-assembly phenomenon.

565 Furthermore, the surface charge of the particles has been determined. The particles surface
566 was negatively charged and the corresponding electrophoretic mobility was equal to $-3.062 \pm$
567 $0.039 \mu\text{m.cm/V.s}$ (approx. Zeta potential : $-39.1 \pm 0.5 \text{ mV}$) (pH of the sample : 6.23 ± 0.12).
568 The GA electrophoretic mobility was measured at $-2.492 \pm 0.091 \mu\text{m.cm/V.s}$ (approx. Zeta
569 potential : $-31.8 \pm 1.1 \text{ mV}$). This negative charge could prevent aggregation although the large
570 particle size lead to rapid sedimentation. A simple agitation then allowed the particles to be
571 resuspended.

572

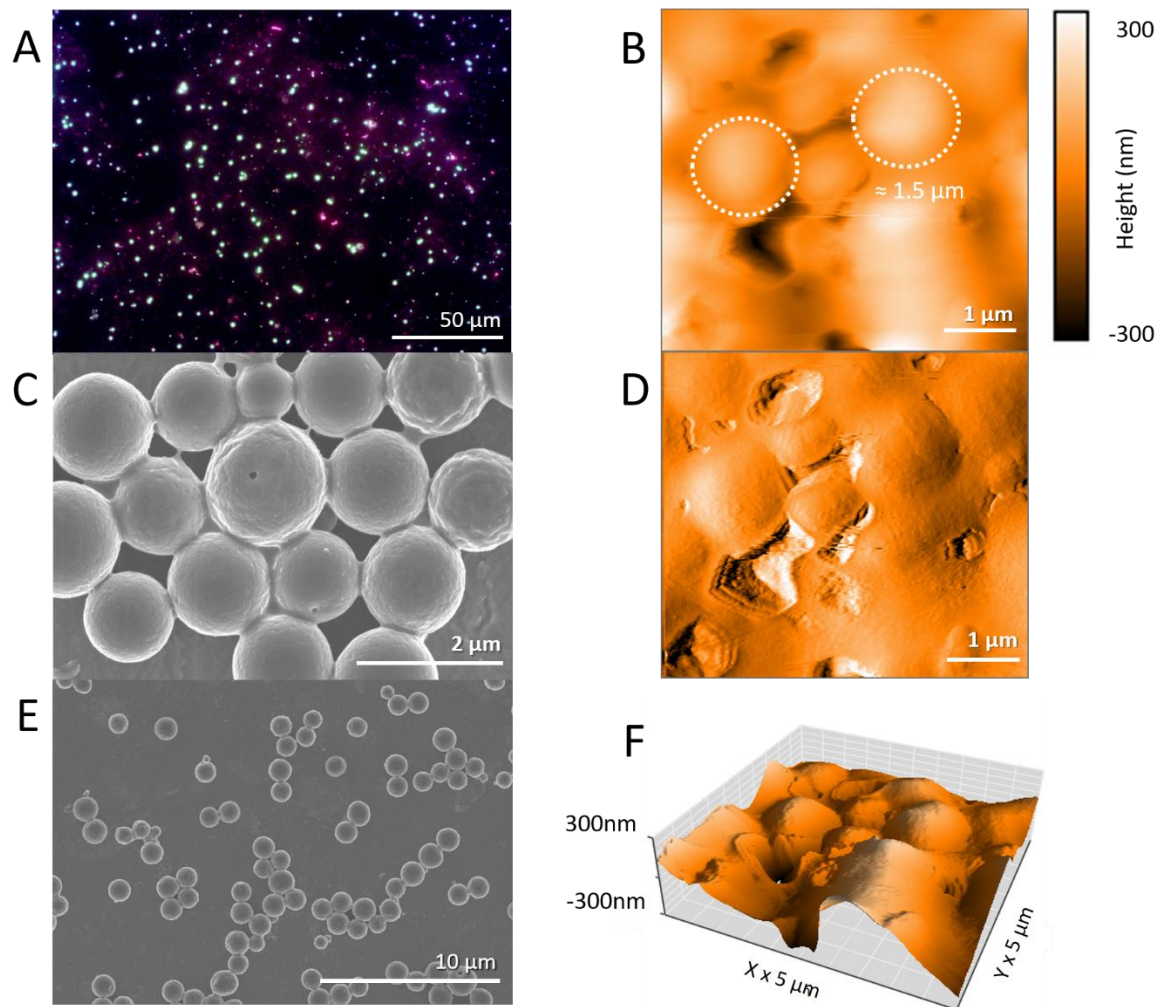


573

574 Figure 6 : Size distribution expressed in intensity (solid blue line), volume (red dash dot line)
575 and number (blue dash dot line), of GAC dispersed in water at 0.005% w/v

576 3.7 Morphological study

577 In order to investigate further the self-assembly behaviour of the modified gum Arabic in
578 water, the structure of the obtained particles had been studied by several microscopic technics.
579 Obtained micrographs are shown in Figure 7. Epifluorescence microscopy images Figure 7A
580 confirmed the presence of the OXP, that emit fluorescence from spherical particles. SEM
581 (Figure 7C and E) confirmed the spherical shape of the particles. These particles presented a
582 relatively smooth surface which was also observed by AFM topography measurements where
583 particles presented a roughness of 24.50 ± 9.87 nm (Figure 7B, D and F). Size determined
584 from the SEM micrograph analysis revealed the majority particles size was of 1.1 μm and
585 AFM images showed a size below 1.5 μm , which was smaller than the one determined from
586 DLS measurement. This was consistent since DLS measures the hydrodynamic radius of the
587 particles, which includes a hydration layer. It is also possible that drying induces a slight
588 contraction of the particles due to water loss.



589

590 Figure 7: Micrographs obtained by (A) fluorescence microscopy magnification $\times 400$, AFM:
 591 (B) height image (D) deflection view (F) 3D view and SEM magnification (C) $\times 20,000$ and
 592 (D) $\times 5,000$

593

594 Additionally, the elastic modulus of the GAC particles was evaluated by AFM
 595 nanoindentation (see Figure S2 in supplementary materials) and a value of 38 ± 9 MPa was
 596 recorded. This value may seem high if compared to alginate microbead (about 300 μm)
 597 which has an elastic modulus slightly lower than 3 kPa (Chui, Bonilla-Brunner, Seifert,
 598 Contera, & Ye, 2019). The assemblies were therefore rather strong, which may explain their
 599 good resistance to drying imposed by the microscopy techniques used.

600 4. Conclusions

601 In this study, the modification of gum Arabic by an enzymatic process led to the addition
602 of curcumin oxidation products to its structure which was confirmed by infrared
603 spectroscopy. Ester bonds were created between GA and the products resulting from the
604 oxidation of curcumin by the laccase. The polysaccharide molecular weight determined by
605 SEC-MALS was greatly increased. The presence of these OXP modifies the properties of the
606 polysaccharide. Indeed, the presence of these new compounds in the GAC structure have
607 increased the antioxidant activity of the gum by 25,000 times. From DSC measurements, the
608 grafting of the curcumin OXP entities induced a plasticizing effect and lead to a lowering of
609 the polymer glass transition temperature to 51 °C. A lowering of the polysaccharide
610 hygroscopy and hydrophily was also reported. The modification changed then the GA
611 hydrophobicity/hydrophobicity balance. This change allows the GAC to obtain a greater
612 capacity to decrease the surface tension of water than the GA until 51.6 mN.m⁻¹ compared to
613 65 mN.m⁻¹ for the native polymer at a polymer concentration in water of 0.5% (wt). As a
614 result of these modifications, GAC became able to form spontaneously spherical particles of
615 about 1.6 µm in aqueous solution with a very low polydispersity. It denotes the change of
616 properties of the gum in water since it is naturally very polydisperse. It is therefore interesting
617 to see that the modification by OXP of curcumin allowed to pass from a very soluble and
618 polydispersed polymer (Atgié, Garrigues, Chennevière, Masbernat, & Roger, 2019; Renard et
619 al., 2006) to an insoluble and quite monodispersed polymer at the same concentrations. It
620 would be very interesting to study more in depth the characteristics of the assemblies such as
621 defining the critical aggregation concentration or to study the impact of the physicochemical
622 properties of the medium on the formed particles. It could also be very interesting to carry out
623 encapsulation tests.

624 **5. Acknowledgments**

625 The authors acknowledge support of the LIBio by the "Impact Biomolecules" project of the
626 "Lorraine Université d'Excellence" (Investissements d'avenir – ANR).

627 The authors acknowledge support of the CPER Agrovalor.

628 We would like to thank Nexira for kindly providing the gum Arabic used in this article.

629 We would like to thank Novozymes for kindly providing the laccase used in this article.

630 We also thank Aurelie Seiler for the technical support.

631 **6. Declaration of interest**

632 Declarations of interest: none

633 **7. Author contribution**

634 Aurélie A. ADAM: Conceptualization; Formal analysis; Investigation; Data curation; Writing
635 original draft

636 Jordane Jasniewski: Conceptualization; Investigation; Validation; Data curation; Supervision;
637 Writing - reviewing & editing

638 Marie E. Vuillemin: Reviewing

639 Blandine Simard: Investigation; Data curation

640 Jennifer Burgain: Investigation; Data curation

641 Régis Badin: Investigation; Data curation

642 Lionel Muniglia: Validation & reviewing

643 Florentin Michaux: Conceptualization; Validation; Data curation; Supervision; Writing -
644 reviewing & editing

645 **8. References**

646 Abdul Rohman, Sudjadi, Dwiky Devi, and Ardi Dwiky Ramadhani. 2015. 'Analysis of
647 Curcumin in Curcuma Longa and Curcuma Xanthorriza Using FTIR Spectroscopy and
648 Chemometrics'. *Research Journal of Medicinal Plant* 9 (4): 179–86.
649 <https://doi.org/10.3923/rjmp.2015.179.186>.

650 Ahmad, Syed Ishraque, Nasreen Mazumdar, and Sunil Kumar. 2013. 'Functionalization of
651 Natural Gum: An Effective Method to Prepare Iodine Complex'. *Carbohydrate*
652 *Polymers* 92 (1): 497–502. <https://doi.org/10.1016/j.carbpol.2012.09.049>.

653 Akiyoshi, K., and J. Sunamoto. 1996. 'Supramolecular Assembly of Hydrophobized
654 Polysaccharides'. *Supramolecular Science* 3 (1–3): 157–63.
655 [https://doi.org/10.1016/0968-5677\(96\)00031-4](https://doi.org/10.1016/0968-5677(96)00031-4).

- 656 Aljawish, Abdulhadi, Isabelle Chevalot, Jordane Jasniewski, Anne-Marie Revol-Junelles, Joël
657 Scher, and Lionel Muniglia. 2014. ‘Laccase-Catalysed Functionalisation of Chitosan
658 by Ferulic Acid and Ethyl Ferulate: Evaluation of Physicochemical and Biofunctional
659 Properties’. *Food Chemistry* 161 (October): 279–87.
660 <https://doi.org/10.1016/j.foodchem.2014.03.076>.
- 661 Aljawish, Abdulhadi, Isabelle Chevalot, Bernadette Piffaut, Corinne Rondeau-Mouro, Michel
662 Girardin, Jordane Jasniewski, Joël Scher, and Lionel Muniglia. 2012.
663 ‘Functionalization of Chitosan by Laccase-Catalyzed Oxidation of Ferulic Acid and
664 Ethyl Ferulate under Heterogeneous Reaction Conditions’. *Carbohydrate Polymers* 87
665 (1): 537–44. <https://doi.org/10.1016/j.carbpol.2011.08.016>.
- 666 Aljawish, Abdulhadi, Lionel Muniglia, Amira Klouj, Jordane Jasniewski, Joël Scher, and
667 Stephane Desobry. 2016. ‘Characterization of Films Based on Enzymatically
668 Modified Chitosan Derivatives with Phenol Compounds’. *Food Hydrocolloids* 60
669 (October): 551–58. <https://doi.org/10.1016/j.foodhyd.2016.04.032>.
- 670 Aphibanthammakit, Chutima, Michaël Nigen, Sébastien Gaucel, Christian Sanchez, and
671 Pascale Chalier. 2018. ‘Surface Properties of Acacia Senegal vs Acacia Seyal Films
672 and Impact on Specific Functionalities’. *Food Hydrocolloids* 82 (September): 519–33.
673 <https://doi.org/10.1016/j.foodhyd.2018.04.032>.
- 674 Atgié, M., J.C. Garrigues, Alexis Chennevière, O. Masbernat, and K. homogenous. 2019.
675 ‘Gum Arabic in Solution: Composition and Multi-Scale Structures’. *Food*
676 *Hydrocolloids* 91 (June): 319–30. <https://doi.org/10.1016/j.foodhyd.2019.01.033>.
- 677 Božič, Mojca, Selestina Gorgieva, and Vanja Kokol. 2012a. ‘Laccase-Mediated
678 Functionalization of Chitosan by Caffeic and Gallic Acids for Modulating Antioxidant
679 and Antimicrobial Properties’. *Carbohydrate Polymers* 87 (4): 2388–98.
680 <https://doi.org/10.1016/j.carbpol.2011.11.006>.
- 681 ———. 2012b. ‘Homogeneous and Heterogeneous Methods for Laccase-Mediated
682 Functionalization of Chitosan by Tannic Acid and Quercetin’. *Carbohydrate Polymers*
683 89 (3): 854–64. <https://doi.org/10.1016/j.carbpol.2012.04.021>.
- 684 Cao, Chong, Lu Zhang, Xiao-Xi Zhang, and Feng-Pei Du. 2013. ‘Effect of Gum Arabic on
685 the Surface Tension and Surface Dilational Rheology of Trisiloxane Surfactant’. *Food*
686 *Hydrocolloids* 30 (1): 456–62. <https://doi.org/10.1016/j.foodhyd.2012.07.006>.
- 687 Chatjigakis, A.K, C Pappas, N.Proxenia, O.Kalantzi, P.Rodis, and M Polissiou. 1998. ‘FT-IR
688 Spectroscopic Determination of the Degree of Esterification of Cell Wall Pectins from
689 Stored Peaches and Correlation to Textural Changes’. *Carbohydrate Polymers* 37 (4):
690 395–408. [https://doi.org/10.1016/S0144-8617\(98\)00057-5](https://doi.org/10.1016/S0144-8617(98)00057-5).
- 691 Chui, Chih-Yao, Andrea Bonilla-Brunner, Jacob Seifert, Sonia Contera, and Hua Ye. 2019.
692 ‘Atomic Force Microscopy-Indentation Demonstrates That Alginate Beads Are
693 Mechanically Stable under Cell Culture Conditions’. *Journal of the Mechanical*
694 *Behavior of Biomedical Materials* 93 (May): 61–69.
695 <https://doi.org/10.1016/j.jmbbm.2019.01.019>.
- 696 Cozic, Céline, Luc Picton, Marie-Rose Garda, Franck Marlhoux, and Didier Le Cerf. 2009.
697 ‘Analysis of Arabic Gum: Study of Degradation and Water Desorption Processes’.
698 *Food Hydrocolloids* 23 (7): 1930–34. <https://doi.org/10.1016/j.foodhyd.2009.02.009>.
- 699 Curcio, Manuela, Giuseppe Cirillo, Paola Tucci, Annafranca Farfalla, Emilia Bevacqua,
700 Orazio Vittorio, Francesca Iemma, and Fiore Pasquale Nicoletta. 2019. ‘Dextran-

- 701 Curcumin Nanoparticles as a Methotrexate Delivery Vehicle: A Step Forward in
702 Breast Cancer Combination Therapy'. *Pharmaceuticals* 13 (1): 2.
703 <https://doi.org/10.3390/ph13010002>.
- 704 Dickinson, Eric, Brent S. Murray, George Stainsby, and Douglas M.W. Anderson. 1988.
705 'Surface Activity and Emulsifying Behaviour of Some Acacia Gums'. *Food*
706 *Hydrocolloids* 2 (6): 477–90. [https://doi.org/10.1016/S0268-005X\(88\)80047-X](https://doi.org/10.1016/S0268-005X(88)80047-X).
- 707 Ebrahimi, Behzad, Aziz Homayouni Rad, Babak Ghanbarzadeh, Torbati Mohammadali, and
708 Falcone Pasquale M. 2020. 'The Emulsifying and Foaming Properties of Amuniacum
709 Gum (Dorema Ammoniacum) in Comparison with Gum Arabic | EndNote Click'.
710 2020.
711 [https://click.endnote.com/viewer?doi=10.1002%2Ffsn3.1658&token=WzIxOTg3Nzgs](https://click.endnote.com/viewer?doi=10.1002%2Ffsn3.1658&token=WzIxOTg3NzgsIjEwLjEwMDIvZnNuMy4xNjU4Il0.oVeHd9FwBRzqRdFvh-9ew1ZTFOA)
712 [IjEwLjEwMDIvZnNuMy4xNjU4Il0.oVeHd9FwBRzqRdFvh-9ew1ZTFOA](https://click.endnote.com/viewer?doi=10.1002%2Ffsn3.1658&token=WzIxOTg3NzgsIjEwLjEwMDIvZnNuMy4xNjU4Il0.oVeHd9FwBRzqRdFvh-9ew1ZTFOA).
- 713 Frascareli, Elen Cristina, Vanessa Martins Silva, Renata Valeriano Tonon, and Míriam Dupas
714 Hubinger. 2012. 'Determination of Critical Storage Conditions of Coffee Oil
715 Microcapsules by Coupling Water Sorption Isotherms and Glass Transition
716 Temperature'. *International Journal of Food Science & Technology* 47 (5): 1044–54.
717 <https://doi.org/10.1111/j.1365-2621.2012.02939.x>.
- 718 Grein, Aline, Bruno C. da Silva, Cinthia F. Wendel, Cesar A. Tischer, Maria Rita
719 Sierakowski, Angela B. Dewes Moura, Marcello Iacomini, Philip A.J. Gorin,
720 Fernanda F. Simas-Tosin, and Izabel C. Riegel-Vidotti. 2013. 'Structural
721 Characterization and Emulsifying Properties of Polysaccharides of Acacia Mearnsii de
722 Wild Gum'. *Carbohydrate Polymers* 92 (1): 312–20.
723 <https://doi.org/10.1016/j.carbpol.2012.09.041>.
- 724 Hamdani, Afshan Mumtaz, Idrees Ahmed Wani, Naseer Ahmad Bhat, and F.A. Masoodi.
725 2018. 'Chemical Composition, Total Phenolic Content, Antioxidant and
726 Antinutritional Characterisation of Exudate Gums'. *Food Bioscience* 23 (June): 67–
727 74. <https://doi.org/10.1016/j.fbio.2018.03.006>.
- 728 Hasan, M, G. Ben Messaoud, F. Michaux, A. Tamayol, C.J.F. Kahn, M. Linder, and E. Arab-
729 Tehrani. 2016. 'Chitosan-Coated Liposomes Encapsulating Curcumin: Study of
730 Lipid–Polysaccharide Interactions and Nanovesicle Behavior'. *RSC Advances*, 15.
- 731 Hou, Chuchu, Shengfang Wu, Yongmei Xia, Glyn O. Phillips, and Steve W. Cui. 2017. 'A
732 Novel Emulsifier Prepared from Acacia Seyal Polysaccharide through Maillard
733 Reaction with Casein Peptides'. *Food Hydrocolloids* 69 (August): 236–41.
734 <https://doi.org/10.1016/j.foodhyd.2017.01.038>.
- 735 Huie, Jiyun C. 2003. 'Guided Molecular Self-Assembly: A Review of Recent Efforts'. *Smart*
736 *Materials and Structures* 12 (2): 264–71. <https://doi.org/10.1088/0964-1726/12/2/315>.
- 737 Karaki, Nadine, A. Aljawish, L. Muniglia, S. Bouguet-Bonnet, S. Leclerc, C. Paris, J.
738 Jasniewski, and C. Humeau-Virot. 2017. 'Functionalization of Pectin with Laccase-
739 Mediated Oxidation Products of Ferulic Acid'. *Enzyme and Microbial Technology* 104
740 (September): 1–8. <https://doi.org/10.1016/j.enzmictec.2017.05.001>.
- 741 Karaki, Nadine, Abdulhadi Aljawish, Catherine Humeau, Lionel Muniglia, and Jordane
742 Jasniewski. 2016. 'Enzymatic Modification of Polysaccharides: Mechanisms,
743 Properties, and Potential Applications: A Review'. *Enzyme and Microbial Technology*
744 90 (August): 1–18. <https://doi.org/10.1016/j.enzmictec.2016.04.004>.

- 745 Karaki, Nadine, Abdulhadi Aljawish, Lionel Muniglia, Catherine Humeau, and Jordane
746 Jasniewski. 2016. 'Physicochemical Characterization of Pectin Grafted with
747 Exogenous Phenols'. *Food Hydrocolloids* 60 (October): 486–93.
748 <https://doi.org/10.1016/j.foodhyd.2016.04.004>.
- 749 Kumar, Guneet, Paul J. Smith, and Gregory F. Payne. 1999. 'Enzymatic Grafting of a Natural
750 Product onto Chitosan to Confer Water Solubility under Basic Conditions'.
751 *Biotechnology and Bioengineering* 63 (2): 154–65.
752 [https://doi.org/10.1002/\(SICI\)1097-0290\(19990420\)63:2<154::AID-BIT4>3.0.CO;2-
R](https://doi.org/10.1002/(SICI)1097-0290(19990420)63:2<154::AID-BIT4>3.0.CO;2-
753 R).
- 754 Li, Shijie, Qingping Xiong, Xiaoping Lai, Xia Li, Mianjie Wan, Jingnian Zhang, Yajuan Yan,
755 et al. 2016. 'Molecular Modification of Polysaccharides and Resulting Bioactivities'.
756 *Comprehensive Reviews in Food Science and Food Safety* 15 (2): 237–50.
757 <https://doi.org/10.1111/1541-4337.12161>.
- 758 Liu, Xiaocui, Lijun You, Solaiman Tarafder, Lin Zou, Zhexiang Fang, Jingdi Chen, Chang
759 Hun Lee, and Qiqing Zhang. 2019. 'Curcumin-Releasing Chitosan/Aloe Membrane
760 for Skin Regeneration'. *Chemical Engineering Journal* 359 (March): 1111–19.
761 <https://doi.org/10.1016/j.cej.2018.11.073>.
- 762 Liu, Yujia, Yanxue Cai, Xueying Jiang, Jinping Wu, and Xueyi Le. 2016. 'Molecular
763 Interactions, Characterization and Antimicrobial Activity of Curcumin–Chitosan
764 Blend Films'. *Food Hydrocolloids* 52 (January): 564–72.
765 <https://doi.org/10.1016/j.foodhyd.2015.08.005>.
- 766 Liu, Yujia, Danyang Ying, Yanxue Cai, and Xueyi Le. 2017. 'Improved Antioxidant Activity
767 and Physicochemical Properties of Curcumin by Adding Ovalbumin and Its Structural
768 Characterization'. *Food Hydrocolloids* 72 (November): 304–11.
769 <https://doi.org/10.1016/j.foodhyd.2017.06.007>.
- 770 Lopez-Torrez, Lizeth, Michaël Nigen, Pascale Williams, Thierry Doco, and Christian
771 Sanchez. 2015. 'Acacia Senegal vs. Acacia Seyal Gums – Part 1: Composition and
772 Structure of Hyperbranched Plant Exudates'. *Food Hydrocolloids* 51 (October): 41–
773 53. <https://doi.org/10.1016/j.foodhyd.2015.04.019>.
- 774 Lykiema, J, K S W Sing, J Haber, M Kerker, E Wolfram, J H Block, N V Churaev, et al.
775 1984. 'Reporting Physiosorption Data Fot Gas/Solid Systems', 17.
- 776 Masuelli, Martin A. 2013. 'Hydrodynamic Properties of Whole Arabic Gum'. *American
777 Journal of Food Science and Technology* 1 (3): 60–66.
- 778 Mortensen, Alicja, Fernando Aguilar, Riccardo Crebelli, Alessandro Di Domenico, Maria
779 Jose Frutos, Pierre Galtier, David Gott, et al. 2017. 'Re-Evaluation of Acacia Gum (E
780 414) as a Food Additive'. *EFSA Journal* 15 (4): e04741.
781 <https://doi.org/10.2903/j.efsa.2017.4741>.
- 782 Mothé, C.G, and M.A Rao. 2000. 'Thermal Behavior of Gum Arabic in Comparison with
783 Cashew Gum'. *Thermochimica Acta* 357–358 (August): 9–13.
784 [https://doi.org/10.1016/S0040-6031\(00\)00358-0](https://doi.org/10.1016/S0040-6031(00)00358-0).
- 785 Mundlia, Jyoti, Munish Ahuja, Pradeep Kumar, and Viness Pillay. 2019. 'Pectin–Curcumin
786 Composite: Synthesis, Molecular Modeling and Cytotoxicity'. *Polymer Bulletin* 76
787 (6): 3153–73. <https://doi.org/10.1007/s00289-018-2538-0>.
- 788 Nakauma, Makoto, Takahiro Funami, Sakie Noda, Sayaka Ishihara, Saphwan Al-Assaf,
789 Katsuyoshi Nishinari, and Glyn O. Phillips. 2008. 'Comparison of Sugar Beet Pectin,

- 790 Soybean Soluble Polysaccharide, and Gum Arabic as Food Emulsifiers. 1. Effect of
791 Concentration, PH, and Salts on the Emulsifying Properties'. *Food Hydrocolloids* 22
792 (7): 1254–67. <https://doi.org/10.1016/j.foodhyd.2007.09.004>.
- 793 Nascimento da Silva, Milena, Jéssica de Matos Fonseca, Helena Kirchner Feldhaus, Lenilton
794 Santos Soares, Germán Ayala Valencia, Carlos Eduardo Maduro de Campos, Marco
795 Di Luccio, and Alcilene Rodrigues Monteiro. 2019. 'Physical and Morphological
796 Properties of Hydroxypropyl Methylcellulose Films with Curcumin Polymorphs'.
797 *Food Hydrocolloids* 97 (December): 105217.
798 <https://doi.org/10.1016/j.foodhyd.2019.105217>.
- 799 Osman, Mohamed E., Peter A. Williams, Alan R. Menzies, and Glyn O. Phillips. 1993.
800 'Characterization of Commercial Samples of Gum Arabic'. *Journal of Agricultural
801 and Food Chemistry* 41 (1): 71–77. <https://doi.org/10.1021/jf00025a016>.
- 802 Peng, Shengfeng, Ziling Li, Liqiang Zou, Wei Liu, Chengmei Liu, and David Julian
803 McClements. 2018. 'Improving Curcumin Solubility and Bioavailability by
804 Encapsulation in Saponin-Coated Curcumin Nanoparticles Prepared Using a Simple
805 PH-Driven Loading Method'. *Food & Function* 9 (3): 1829–39.
806 <https://doi.org/10.1039/C7FO01814B>.
- 807 Pérez-Alonso, C., C.I. Beristain, C. Lobato-Calleros, M.E. Rodríguez-Huezo, and E.J.
808 Vernon-Carter. 2006. 'Thermodynamic Analysis of the Sorption Isotherms of Pure
809 and Blended Carbohydrate Polymers'. *Journal of Food Engineering* 77 (4): 753–60.
810 <https://doi.org/10.1016/j.jfoodeng.2005.08.002>.
- 811 Pirestani, Safoura, Ali Nasirpour, Javad Keramat, Stéphane Desobry, and Jordane Jasniewski.
812 2017. 'Effect of Glycosylation with Gum Arabic by Maillard Reaction in a Liquid
813 System on the Emulsifying Properties of Canola Protein Isolate'. *Carbohydrate
814 Polymers* 157 (February): 1620–27. <https://doi.org/10.1016/j.carbpol.2016.11.044>.
- 815 Poljanšek, Ida, Urška Šebenik, and Matjaž Krajnc. 2006. 'Characterization of Phenol–Urea–
816 Formaldehyde Resin by Inline FTIR Spectroscopy'. *Journal of Applied Polymer
817 Science* 99 (5): 2016–28. <https://doi.org/10.1002/app.22161>.
- 818 Randall, R.C., G.O. Phillips, and P.A. Williams. 1988. 'The Role of the Proteinaceous
819 Component on the Emulsifying Properties of Gum Arabic'. *Food Hydrocolloids* 2 (2):
820 131–40. [https://doi.org/10.1016/S0268-005X\(88\)80011-0](https://doi.org/10.1016/S0268-005X(88)80011-0).
- 821 Renard, D., C. Garnier, A. Lapp, C. Schmitt, and C. Sanchez. 2012. 'Structure of
822 Arabinogalactan-Protein from Acacia Gum: From Porous Ellipsoids to
823 Supramolecular Architectures'. *Carbohydrate Polymers* 90 (1): 322–32.
824 <https://doi.org/10.1016/j.carbpol.2012.05.046>.
- 825 Renard, Denis, Laurence Lavenant-Gourgeon, Marie-Christine Ralet, and Christian Sanchez.
826 2006. 'Acacia Senegal Gum: Continuum of Molecular Species Differing by Their
827 Protein to Sugar Ratio, Molecular Weight, and Charges'. *Biomacromolecules* 7 (9):
828 2637–49. <https://doi.org/10.1021/bm060145j>.
- 829 Sabet, Saman, Ali Rashidinejad, Laurence D. Melton, Zoran Zujovic, Alireza Akbarinejad,
830 Michel Nieuwoudt, Chris K. Seal, and Duncan J. McGillivray. 2021. 'The Interactions
831 between the Two Negatively Charged Polysaccharides: Gum Arabic and Alginate'.
832 *Food Hydrocolloids* 112 (March): 106343.
833 <https://doi.org/10.1016/j.foodhyd.2020.106343>.

- 834 Sanchez, C., M. Nigen, V. Mejia Tamayo, T. Doco, P. Williams, C. Amine, and D. Renard.
835 2018. 'Acacia Gum: History of the Future'. *Food Hydrocolloids* 78 (May): 140–60.
836 <https://doi.org/10.1016/j.foodhyd.2017.04.008>.
- 837 Sanchez, Christian, Denis Renard, Paul Robert, Christophe Schmitt, and Jacques Lefebvre.
838 2002. 'Structure and Rheological Properties of Acacia Gum Dispersions'. *Food*
839 *Hydrocolloids* 16 (3): 257–67. [https://doi.org/10.1016/S0268-005X\(01\)00096-0](https://doi.org/10.1016/S0268-005X(01)00096-0).
- 840 Sarika, P.R., Nirmala Rachel James, P.R. Anil Kumar, Deepa K. Raj, and T.V. Kumary. 2015.
841 'Gum Arabic-Curcumin Conjugate Micelles with Enhanced Loading for Curcumin
842 Delivery to Hepatocarcinoma Cells'. *Carbohydrate Polymers* 134 (December): 167–
843 74. <https://doi.org/10.1016/j.carbpol.2015.07.068>.
- 844 Six, Jean-Luc, and Khalid Ferji. 2019. 'Polymerization Induced Self-Assembly: An
845 Opportunity toward the Self-Assembly of Polysaccharide-Containing Copolymers into
846 High-Order Morphologies'. *Polymer Chemistry* 10 (1): 45–53.
847 <https://doi.org/10.1039/C8PY01295D>.
- 848 Spizzirri, U. Gianfranco, Ortensia Ilaria Parisi, Francesca Iemma, Giuseppe Cirillo, Francesco
849 Puoci, Manuela Curcio, and Nevio Picci. 2010. 'Antioxidant–Polysaccharide
850 Conjugates for Food Application by Eco-Friendly Grafting Procedure'. *Carbohydrate*
851 *Polymers* 79 (2): 333–40. <https://doi.org/10.1016/j.carbpol.2009.08.010>.
- 852 Tahir, Haroon Elrasheid, Zou Xiaobo, Shi Jiyong, Gustav Komla Mahunu, Xiaodong Zhai,
853 and Abdalbasit Adam Mariod. 2018. 'Quality and Postharvest-Shelf Life of Cold-
854 Stored Strawberry Fruit as Affected by Gum Arabic (Acacia Senegal) Edible Coating'.
855 *Journal of Food Biochemistry* 42 (3): e12527. <https://doi.org/10.1111/jfbc.12527>.
- 856 Vasile, Franco Emanuel, María Julia Martinez, Víctor Manuel Pizones Ruiz-Henestrosa,
857 María Alicia Judis, and María Florencia Mazzobre. 2016. 'Physicochemical,
858 Interfacial and Emulsifying Properties of a Non-Conventional Exudate Gum (Prosopis
859 Alba) in Comparison with Gum Arabic'. *Food Hydrocolloids* 56 (May): 245–53.
860 <https://doi.org/10.1016/j.foodhyd.2015.12.016>.
- 861 Verbeken, D., S. Dierckx, and K. Dewettinck. 2003. 'Exudate Gums: Occurrence, Production,
862 and Applications'. *Applied Microbiology and Biotechnology* 63 (1): 10–21.
863 <https://doi.org/10.1007/s00253-003-1354-z>.
- 864 Vuillemin, Marie E., Florentin Michaux, Aurélie A. Adam, Michel Linder, Lionel Muniglia,
865 and Jordane Jasniewski. 2020. 'Physicochemical Characterizations of Gum Arabic
866 Modified with Oxidation Products of Ferulic Acid'. *Food Hydrocolloids*, April,
867 105919. <https://doi.org/10.1016/j.foodhyd.2020.105919>.
- 868 Vuillemin, Marie E., Florentin Michaux, Aurélie Seiler, Michel Linder, Lionel Muniglia, and
869 Jordane Jasniewski. 2021. 'Polysaccharides Enzymatic Modification to Control the
870 Coacervation or the Aggregation Behavior: A Thermodynamic Study'. *Food*
871 *Hydrocolloids*, August, 107092. <https://doi.org/10.1016/j.foodhyd.2021.107092>.
- 872 Wang, Hao, P.A. Williams, and C. Senan. 2014. 'Synthesis, Characterization and
873 Emulsification Properties of Dodecenyl Succinic Anhydride Derivatives of Gum
874 Arabic'. *Food Hydrocolloids* 37 (June): 143–48.
875 <https://doi.org/10.1016/j.foodhyd.2013.10.033>.
- 876 Wu, Y., N.A.M. Eskin, W. Cui, and B. Pokharel. 2015. 'Emulsifying Properties of Water
877 Soluble Yellow Mustard Mucilage: A Comparative Study with Gum Arabic and Citrus

- 878 Pectin'. *Food Hydrocolloids* 47 (May): 191–96.
879 <https://doi.org/10.1016/j.foodhyd.2015.01.020>.
- 880 Zohuriaan, M.J, and F Shokrolahi. 2004. 'Thermal Studies on Natural and Modified Gums'.
881 *Polymer Testing* 23 (5): 575–79. <https://doi.org/10.1016/j.polymeresting.2003.11.001>.
- 882 Zohuriaan- Mehr, Mohammad J., Z. Motazedi, K. Kabiri, and A. Ershad- Langroudi. 2005.
883 'New Super- Absorbing Hydrogel Hybrids from Gum Arabic and Acrylic
884 Monomers'. *Journal of Macromolecular Science, Part A* 42 (12): 1655–66.
885 <https://doi.org/10.1080/10601320500246859>.
- 886